Molecular Cell, Vol. 12, 1077–1086, November, 2003, Copyright ©2003 by Cell Press

Mechanism of 5′-Directed Excision in Human Mismatch Repair

Jochen Genschel[1] and Paul Modrich[1,2,*]
[1]Department of Biochemistry and
[2]Howard Hughes Medical Institute
Box 3711
Duke University Medical Center
Durham, North Carolina 27710

Summary

We have developed a purified system that supports mismatch-dependent 5′→3′ excision. In the presence of RPA, ATP, and a mismatch, MutSα activates 5′→3′ excision by EXOI, and excision terminates after removal of the mispair. MutSα confers high processivity on EXOI, and termination is due to RPA-dependent displacement of this processive complex from the helix and a weak ability of EXOI to reload at the RPA-bound gap in the product, as well as MutSα- and MutLα-dependent suppression of EXOI activity in the absence of a mismatch cofactor. As observed in the purified system, excision directed by a 5′ strand break in HeLa nuclear extract can proceed in the absence of MutLα or PCNA, although 3′ excision in the extract system requires both proteins.

Introduction

Mismatched base pairs, which are produced at significant rates due to DNA polymerase errors, are rectified by mismatch repair. Inactivation of the human mismatch repair pathway confers hypermutability and has been implicated in tumor development. Function of this system depends on a number of activities including MutSα (MSH2•MSH6 heterodimer) and MutSβ (MSH2•MSH3), MutLα (MLH1•PMS2), the PCNA replication clamp, DNA polymerase δ, and the single-stranded DNA binding protein RPA (Kolodner, 1996; Modrich and Lahue, 1996; Jiricny, 1998; Buermeyer et al., 1999; Harfe and Jinks-Robertson, 2000). MutSα, MutSβ, MutLα, and PCNA have been implicated in the initiation of repair, whereas DNA polymerase δ and PCNA have been shown to participate in the repair synthesis step of the reaction.

Information concerning the excision step of the reaction has been limited. Analysis of this step in nuclear extracts of human cells has demonstrated that the strand break that directs repair may be located either 3′ or 5′ to the mismatch and has suggested that the reaction is exonucleolytic; excision tracts extend from the strand break that directs repair and terminate at a number of discrete sites centered about 150 nucleotides beyond the original location of the mispair (Fang and Modrich, 1993; Wang and Hays, 2002). RPA protects the gap resulting from mismatch-provoked excision in crude fractions (Ramilo et al., 2002), and exonuclease I (EXOI) plays an important role in the nuclear extract reaction when repair is directed by a strand break located either 5′ or 3′ to the mispair (Genschel et al., 2002; Wei et al., 2003). This bidirectional requirement for EXOI was unexpected because the enzyme hydrolyzes duplex DNA with a polarity that is exclusively 5′ to 3′ (Szankasi and Smith, 1992; Tishkoff et al., 1997; Wilson et al., 1998). EXOI involvement in bidirectional excision could reflect a structural role for the protein in assembly of a mismatch repair complex or may indicate that it has a catalytic function in 3′ excision (Amin et al., 2001; Genschel et al., 2002).

These in vitro studies are consistent with previous genetic studies that implicated yeast EXOI in mismatch repair (Szankasi and Smith, 1992; Tishkoff et al., 1997; Sokolsky and Alani, 2000; Amin et al., 2001; Tran et al., 2001). Yeast EXOI interacts physically with yMSH2 and yMLH1 (Tishkoff et al., 1997; Tran et al., 2001), and the human EXOI homolog interacts with hMSH2, hMSH3, and hMLH1 (Schmutte et al., 1998, 2001; Tishkoff et al., 1998; Rasmussen et al., 2000; Jager et al., 2001). *EXOI* sequence variants have been reported in hereditary nonpolyposis colon cancer patients (Wu et al., 2001), but a number of these have been shown to be polymorphisms that are present in normal populations (Jagmohan-Changur et al., 2003). However, several *EXOI* sequence variants that confer activity defects (Sun et al., 2002) have been observed only in colorectal cancer patients (Jagmohan-Changur et al., 2003), and *EXOI*$^{-/-}$ mice are prone to lymphoma development (Wei et al., 2003).

The excision step of *E. coli* mismatch repair depends on unwinding by DNA helicase II and degradation of the displaced strand by a single-strand-specific exonuclease (Cooper et al., 1993; Viswanathan et al., 2001). In this system excision is controlled via MutS- and MutL-dependent activation of helicase II at a strand break (Dao and Modrich, 1998). By contrast, the finding that MutSα can activate EXOI-dependent 5′ to 3′ excision on a nicked heteroduplex (Genschel et al., 2002) suggests that excision directed by a 5′ strand discontinuity may be regulated by controlling access of this double-strand exonuclease to a 5′ terminus in the human system. We describe here a mismatch-provoked 5′ to 3′ excision reaction in a purified system comprised of only MutSα, MutLα, EXOI, and RPA. Excision by this system is similar to that observed in nuclear extracts and terminates after mismatch removal.

Results

RPA Enhances MutSα-Dependent EXOI Activation in the Presence of MutLα

We have previously shown that human MutSα activates EXOI on a nicked heteroduplex (Genschel et al., 2002). Excision under these conditions is strictly 5′ to 3′, consistent with reported polarities of the yeast and human EXOI (Szankasi and Smith, 1992; Tishkoff et al., 1997; Wilson et al., 1998). However, this simple reaction is anomalous in two respects. The mismatch dependence of excision by this system is less than that observed in nuclear extracts (Fang and Modrich, 1993; Genschel et

*Correspondence: modrich@biochem.duke.edu

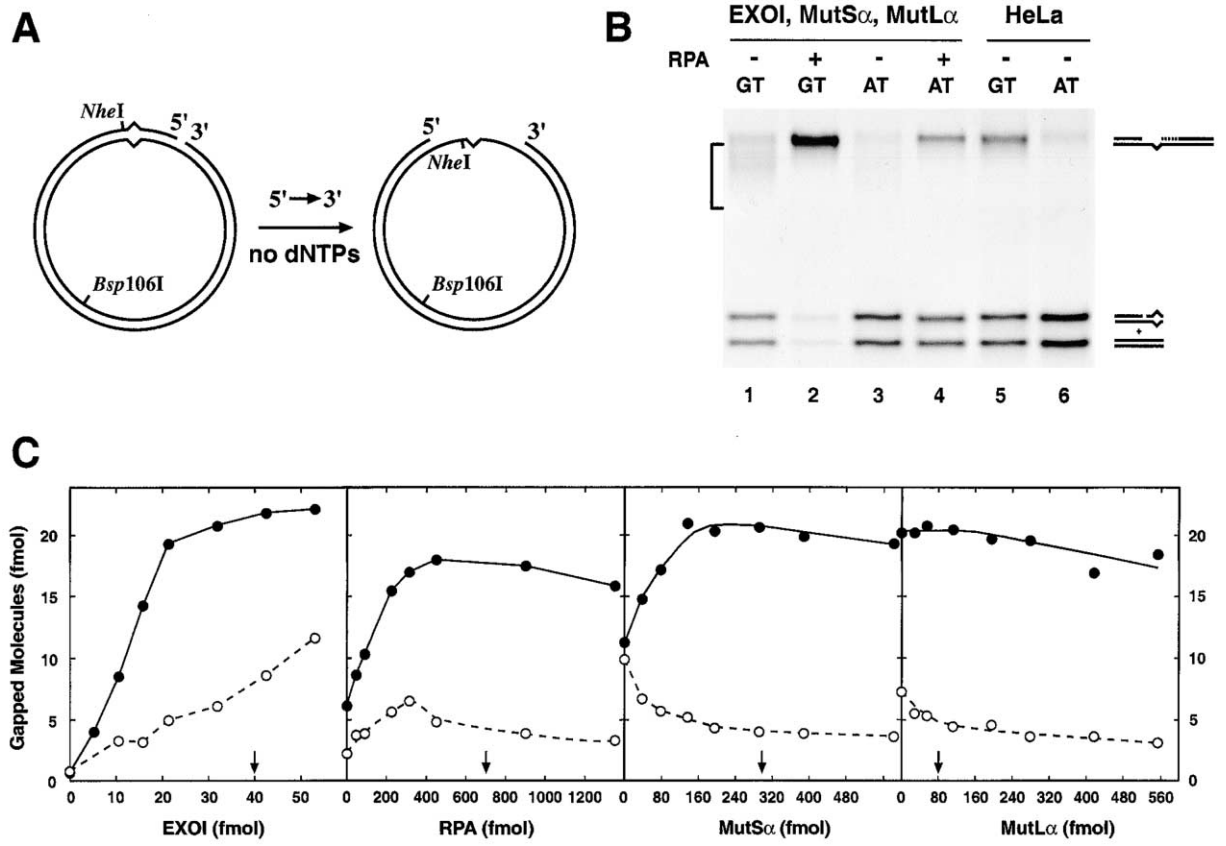

Figure 1. RPA Activates Mismatch-Provoked Excision in a Purified System

(A) Mismatch-provoked excision was scored using 6440 base pair circular f1 DNAs (Fang and Modrich, 1993) containing a G-T mismatch, or an A•T base pair in the otherwise identical homoduplex control, and a site-specific nick in the complementary DNA strand 5′ to the mismatch as viewed along the shorter path joining the two sites. Mismatch-provoked gaps produced in nuclear extract terminate at a number of discrete sites centered about 150 base pairs beyond the mismatch (Fang and Modrich, 1993), rendering the NheI site located 5 base pairs distal to the mismatch resistant to cleavage (Genschel et al., 2002). Cleavage of native substrates with NheI and Bsp106I yields the two rapidly migrating fragments shown diagrammatically to the right of (B). Due to their NheI resistance, excision products scored by NheI-Bsp106I cleavage run as a discrete species on agarose gels with a mobility slightly greater than that of the full-length linear duplex.

(B) Gap formation reactions (Experimental Procedures, lanes 1–4) contained 24 fmol circular nicked A•T homoduplex or G-T heteroduplex (128 base pair nick-mismatch separation distance), 100 ng MutSα (390 fmol), 50 ng MutLα (280 fmol), 5 ng EXOI (53 fmol), and if indicated 100 ng RPA (900 fmol). Reactions shown in lanes 5 and 6 contained 75 μg HeLa nuclear extract instead of purified proteins. After incubation at 37°C for 5 min, DNAs were digested with NheI and Bsp106I, subjected to electrophoresis through a 1% agarose gel, and stained with ethidium bromide. Gap formation that occurs in the purified system in the absence of RPA yields a population of molecules with higher electrophoretic mobilities due to much longer excision tracts (up to several thousand nucleotides; bracket lane 1 and Genschel et al., 2002).

(C) Excision dependence on EXOI, RPA, MutSα, and MutLα. Reactions (Experimental Procedures) contained 24 fmol of incised A•T homoduplex (–○–) or G-T heteroduplex (–●–, 128 base pair separation between nick and mispair), and incubation was 5 min at 37°C. EXOI, RPA, MutSα, and MutLα were varied as shown in the presence of fixed concentrations of the other three components (390 fmol MutSα, 280 fmol MutLα, 900 fmol RPA, and 21 fmol EXOI). Arrows indicate the amount of each protein estimated by quantitative Western blot to be present in 50 μg of nuclear extract, which is the optimal amount for in vitro mismatch repair.

al., 2002; Wang and Hays, 2002), and only a subset of the heteroduplex molecules undergo excision (Genschel et al., 2002). Since RPA, the human single-stranded DNA binding protein, has been implicated in stabilization of mismatch-provoked excision tracts in crude nuclear fractions (Ramilo et al., 2002), we have examined the effects of this protein on the purified system.

The effects of RPA on EXOI-dependent excision are illustrated in Figure 1. As observed previously (Genschel et al., 2002), MutSα, MutLα, and EXOI support excision on a G-T heteroduplex that contains a strand break located 128 base pairs 5′ to the mismatch. However, as noted above, only a fraction of the substrate molecules participate in the reaction, and excision tracts produced under these conditions range in size up to several thousand nucleotides, much longer than the ~300 nucleotide excision tracts produced on this G-T heteroduplex in HeLa nuclear extract (Fang and Modrich, 1993; Genschel et al., 2002; Figure 1B, compare lanes 1 and 5). Supplementation of the MutSα, MutLα, EXOI system with RPA dramatically enhanced excision on the G-T heteroduplex (lane 2). Nearly all of the heteroduplex participated in the reaction in the presence of the four proteins, and the distribution of excision products was much more discrete and similar to that observed in HeLa nuclear extract. As compared to the robust excision in the pure system, only 40% of the heteroduplex molecules were subject to excision in HeLa nuclear extract.

Table 1. ATP Is Required for Mismatch Specificity

	No Nucleotide		ADP		ATP		AMPPNP	
	5′GT	5′AT	5′GT	5′AT	5′GT	5′AT	5′GT	5′AT
	Gap Formation (fmol/5 min)							
EXOI	10.2 (± 1.1)	11.2 (± 1.6)	9.4 (± 1.0)	11.8 (± 0.5)	11.3 (± 1.3)	12.6 (± 2.8)	10.8 (± 3.5)	13.0 (± 1.9)
+ MutSα	7.2 (± 0.8)	10.0 (± 1.1)	14.0 (± 1.0)	13.0 (± 1.4)	**20.5 (± 0.3)**	**8.1 (± 0.7)**	11.0 (± 0.4)	9.5 (± 1.4)
+ MutLα	12.3 (± 2.3)	10.8 (± 2.3)	12.5 (± 3.4)	11.4 (± 3.2)	12.7 (± 1.9)	10.8 (± 1.5)	11.6 (± 1.6)	11.9 (± 1.6)
+ MutSα and MutLα	6.4 (± 0.4)	11.0 (± 0.8)	10.5 (± 1.9)	12.7 (± 0.9)	**18.7 (± 0.7)**	**4.0 (± 0.2)**	10.0 (± 1.3)	8.7 (± 0.5)

Excision (fmol/5 min) was scored by restriction endonuclease assay (Figure 1). Reactions contained 21 fmol EXOI and 900 fmol RPA, in the absence or presence of 280 fmol MutLα and 390 fmol MutSα as indicated. Nucleotide concentration was 1.5 mM. Results shown are the average of three independent determinations ±1 standard deviation.

This effect, which has been observed previously, is due to the fact that about half of the nicked molecules are ligated in the extract and removed from the substrate pool (Fang and Modrich, 1993).

Although an A•T homoduplex supports background hydrolysis by EXOI, heteroduplex specificity of excision in the purified system is substantial. As shown in Figure 1C, RPA preferentially activates EXOI excision on heteroduplex DNA in the presence of MutSα and MutLα. This effect requires MutSα, which not only activates excision on a G-T heteroduplex but also suppresses EXOI action on the homoduplex control in a concentration-dependent manner. MutLα is not required for EXOI activation on the heteroduplex but is necessary for MutSα-dependent suppression of excision on homoduplex DNA, which occurs in a concentration-dependent fashion. MutSα- and MutLα-dependent inhibition of excision on homoduplex DNA is a reproducible effect and has been consistently observed in multiple independent experiments (also see Table 1).

At optimal MutSα, MutLα, and RPA concentrations, the purified system hydrolyzes heteroduplex DNA with a 5-fold preference relative to the homoduplex control in a 5 min reaction, a value similar to the 5- to 8-fold specificity observed for the reaction in HeLa nuclear extract (Figure 1B and Genschel et al., 2002). It is important to note that the optimal levels of these proteins (200–400 fmol MutSα, 200–300 fmol MutLα, 500–900 fmol RPA, and 20–40 fmol EXOI) are similar to their levels in 50 μg of HeLa nuclear extract (arrows, Figure 1C), which is optimal for excision/mismatch repair in the crude system. On the basis of quantitative Western analysis (data not shown), we estimate that 50 μg of nuclear extract contains about 300 fmol MutSα, 80 fmol MutLα, 700 fmol RPA, and 40 fmol EXOI.

ATP Requirement for Mismatch Specificity in the Purified System

MutS and MutL homologs harbor adenine nucleotide binding sites, and ATP hydrolysis has been implicated in the function of these proteins in mismatch repair (Kolodner, 1996; Modrich and Lahue, 1996; Jiricny, 1998; Buermeyer et al., 1999; Harfe and Jinks-Robertson, 2000). We therefore examined the effects of adenine nucleotides on heteroduplex and homoduplex hydrolysis by EXOI in the absence and presence of MutSα and MutLα. In the presence of RPA only, EXOI displayed no significant preference for heteroduplex over homoduplex DNA (Table 1). Supplementation of these two components with MutSα in the presence of ATP preferentially activated excision on the G-T heteroduplex and modestly suppressed activity on homoduplex DNA. ADP and nonhydrolyzable AMPPNP were ineffective in this regard, suggesting that ATP hydrolysis is required for MutSα-dependent activation of the exonuclease. Although MutLα was without significant effect on EXOI excision on heteroduplex DNA, the protein substantially suppressed excision on homoduplex DNA provided that MutSα and ATP were also present, resulting in a heteroduplex preference of about 5-fold, corresponding to the value noted above.

Interestingly, MutSα significantly reduced the heteroduplex preference in the absence of nucleotide, an effect due to preferential inhibition of excision on the G-T DNA. This effect can be understood in terms of known properties of MutSα and the nature of NheI endonuclease assay that was used to score the excision results shown in Table 1. In order to be scored as a positive event by this assay, an excision tract must remove the mismatch and span the NheI site located 5 base pairs distal to the mispair (Figure 1A). Since MutSα forms a long-lived complex with a G-T mismatch in the absence of adenine nucleotides (Blackwell et al., 1998), it seems likely that mismatch-bound MutSα is serving as a physical barrier to EXOI progression, preventing the excision tract from reaching the NheI site. Mismatch-bound bacterial MutS has been previously shown to act as a barrier to exonuclease progression in the absence of nucleotide (Ellis et al., 1994). Although MutSα also binds with high affinity to mismatches in the presence of ADP (Blackwell et al., 1998; Gradia et al., 1999), an inhibitory effect of MutSα on heteroduplex excision was not observed in the presence of this nucleotide (Table 1). This may be due to the fact that although ADP does not significantly alter the affinity of MutSα for a mispair, it dramatically enhances the rates at which the protein binds to and leaves a mismatch. At 25°C and an ionic strength similar to that used here, MutSα dissociates from a G-T heteroduplex with a half-life of about 6 min as compared to a 14 s half-life in the presence of ADP (Blackwell et al., 1998). An alternate explanation for this observation is that ADP occupancy of a MutSα nucleotide binding site may modulate interaction of the protein with EXOI.

In the Presence of RPA, MutSα-Activated EXOI Terminates upon Mismatch Removal

While providing a simple assay for excision, the NheI endonuclease resistance assay used above provides no

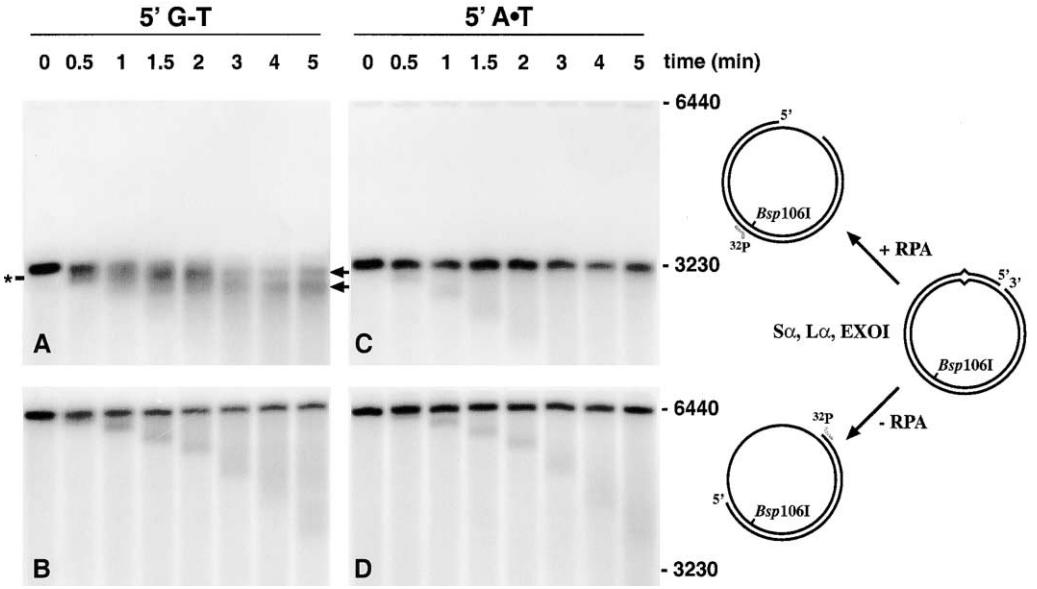

Figure 2. Excision Tract Endpoints

Gap formation reactions with nicked A•T homoduplex or G-T heteroduplex (128 base pair nick-mismatch separation distance) contained per time point 390 fmol MutSα, 280 fmol MutLα, 21 fmol EXOI, and 24 fmol DNA in the presence (A and C) or absence (B and D) of 900 fmol RPA. Products obtained from reactions containing RPA were digested with Bsp106I. DNA samples from reactions in the presence or absence of RPA were subjected to electrophoresis through alkaline agarose and transferred to nylon membranes (Experimental Procedures). For Bsp106I-cleaved products produced in the presence of RPA, membranes were probed with a ^{32}P-labeled oligonucleotide that hybridizes to the processed strand adjacent to the Bsp106I site (gray bar in upper diagram). Products produced in the absence of RPA, which were not digested with Bsp106I, were probed with an oligonucleotide that hybridizes at the 3′ end of the incised strand in the original substrate (gray bar in lower diagram). The two major excision products (arrows) produced with the G-T heteroduplex in the presence of RPA have estimated average lengths of 3040 and 2870 nucleotides. The approximate position of the mismatch is indicated by an asterisk. Control hybridizations (not shown) with an oligonucleotide specific for the other side of the Bsp106I restriction site (upper panel, viral strand coordinates 2508–2527) revealed the presence of a 3′ terminus at or near the location of the strand break in the original substrates.

information on excision tract endpoints. This question was addressed by indirect product end-labeling in time-resolved excision reactions (Fang and Modrich, 1993; Genschel et al., 2002). In the absence of RPA, excision tracts were evident on both heteroduplex and homoduplex DNAs (Figures 2B and 2D). In both cases, only a subset of substrate molecules participated in the reaction, and excision was extensive, removing thousands of nucleotides in 5 min. Supplementation of the MutSα, MutLα, EXOI system with RPA rendered heteroduplex excision much more robust. Under these conditions, essentially all molecules participated in the reaction, and excision terminated after mismatch removal resulting in much shorter tracts. Two major products were observed (arrows, Figure 2A), corresponding to removal of about 190 and 360 nucleotides. Since the G-T mismatch in this heteroduplex is located 128 base pairs from the strand break, excision in the four protein system terminates in the region 60 to 230 nucleotides beyond the location of the mispair, results similar to those obtained with HeLa nuclear extracts where excision terminates at multiple sites centered about 150 nucleotides beyond the mismatch (Fang and Modrich, 1993).

Excision and Excision Intermediates as a Function of Nick-Mismatch Separation Distance

The kinetics of excision on heteroduplex and homoduplex DNAs is shown in Figure 3A as a function of the separation distance between the strand break and the G-T mismatch (or the corresponding A•T base pair in the homoduplex control). The rate at which the excision tract reaches the NheI site located 5 base pairs distal to the mismatch decreases as the nick-mismatch separation distance increases from 128 to 808 base pairs, and initial appearance of NheI-resistant excision products is associated with a lag for separation distances of 494 and 808 base pairs. Nevertheless, mismatch specificity is maintained at the longer separation distances. As in the case of the heteroduplex in which the nick and mismatch are separated by 128 base pairs, EXOI activation on the latter substrates requires MutSα but is MutLα independent (data not shown).

Increase of the nick-mismatch separation distance revealed pseudo-discrete species that appear to be intermediates in heteroduplex hydrolysis in the presence of MutSα, MutLα, and RPA. These species, which are indicated by arrows in Figure 3C and 3D, increase and decrease with time, as expected for reaction intermediates, converging to yield a single major excision product after mismatch removal. Comparison of these hydrolytic intermediates, and the two products shown in Figure 2, indicates that these sequential species differ in size by 250 ± 60 (1 standard deviation) nucleotides. We suggest below that these species are a consequence of EXOI dissociation from excision intermediates during the course of hydrolysis and that such events play a role in the regulation of EXOI hydrolysis.

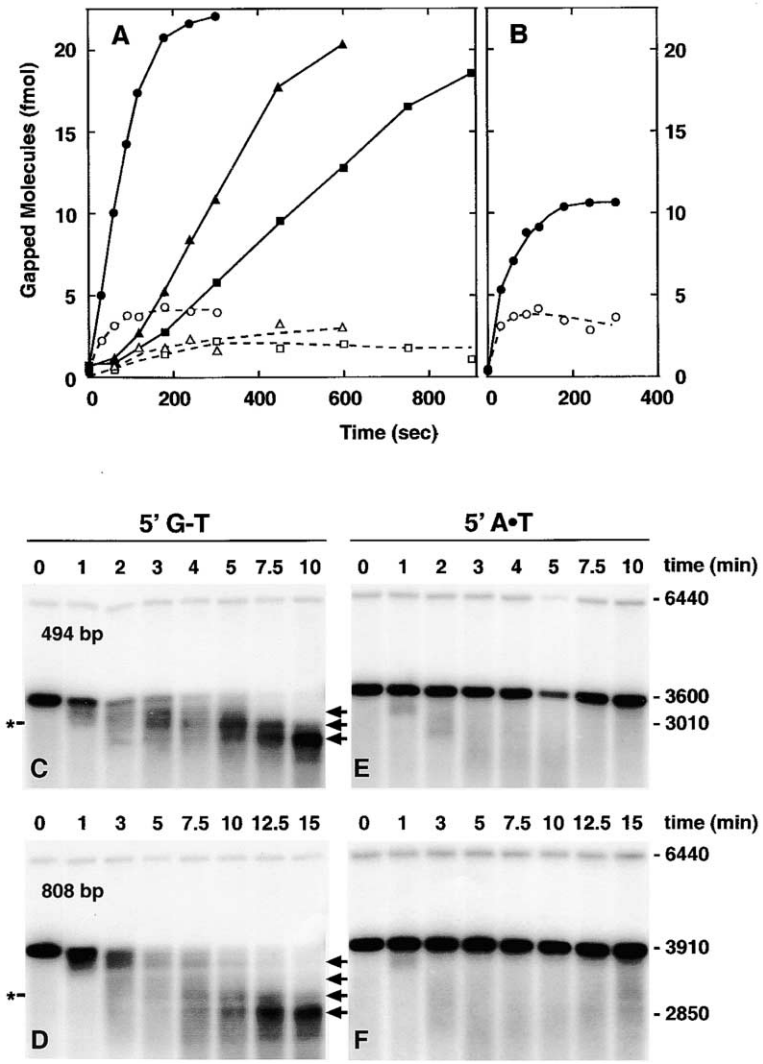

Figure 3. Excision as a Function of Nick-Mismatch Separation

(A) Gap formation reactions contained per time point 390 fmol MutSα, 280 fmol MutLα, 21 fmol EXOI, 900 fmol RPA, and 24 fmol nicked A•T homoduplex (open symbols) or G-T heteroduplex (closed symbols). Kinetics of excision are shown as a function of the distance between the 5′ strand break and the location of the G-T mismatch or control A•T base pair (●, ○ 128 base pairs; ▲, △ 494 base pairs; or ■, □ 808 base pairs). Gap formation was scored by NheI/Bsp106I cleavage assay (Figure 1 and Experimental Procedures).

(B) G-T heteroduplex and A•T homoduplex DNAs with a nick-mismatch separation distance of 128 base pairs subjected to excision as described above except RPA was omitted from the reaction.

(C–F) Excision reactions containing MutSα, MutLα, EXOI, and RPA were performed, and excision intermediates were visualized by indirect end-labeling after Bsp106I cleavage as described in Figure 2. G-T heteroduplexes (C and D) and A•T homoduplexes (E and F) contained a nick in the complementary DNA strand located 494 (C and E) or 808 (D and F) base pairs 5′ to the G-T mispair. The approximate location of the mismatch in each heteroduplex is indicated by an asterisk. Pseudo-discrete species that occur during the course of excision are indicated by arrows. As described in the text, these intermediates may result from dissociation of the 5′ to 3′ excision complex during the course of the reaction.

Some background excision was observed on the A•T homoduplex control DNA in the presence of RPA (Figures 2C, 3E, and 3F), consistent with results obtained with the NheI endonuclease assay described above. We have shown previously that the denaturation-reannealing procedure used for preparation of heteroduplex and control homoduplex DNAs results in the presence of lesions in about 10% of the homoduplex molecules and that these lesions are capable of triggering the bacterial mismatch repair system (Au et al., 1992). Although it is not clear whether these lesions are due to damage introduced during substrate preparation or to natural variation in DNA populations used, it is likely that some of the background excision observed on A•T homoduplex controls is due to this effect. Since the lesions in question are expected to be distributed randomly throughout the homoduplex, defined termination sites would not be observed in this case.

Mechanism of EXOI Modulation by RPA

Figures 3A and 3B illustrate the effect of RPA on kinetics of EXOI excision on hetero- and homoduplex DNAs. The effect of the single-stranded DNA binding protein on the reaction becomes apparent only after an initial phase of product formation. It is important to note that the nature of heteroduplex excision in the presence and absence of RPA visualized by end-labeling (Figures 2A and 2B) is consistent with the kinetics of excision determined by NheI cleavage assay (Figures 3A and 3B). Thus, the kinetics of excision and the nature of excision intermediates produced in the presence or absence of RPA is similar during the first minute of reaction. In the absence of the single-stranded DNA binding protein, subsequent excision is largely directed to molecules that were gapped during the initial phase of the reaction, resulting in their preferential degradation. However, in the presence of RPA, excision is restricted to the region of heteroduplex that contains the nick and the mispair, and the system turns over in the sense that all of the substrate molecules participate in the reaction. These observations suggest that RPA suppresses EXOI excision on gapped DNA after mismatch removal.

This idea was confirmed by the experiments shown in Figure 4, which examine the effects of RPA on production of EXOI hydrolytic intermediates on nicked and gapped DNA. In the absence of MutSα and MutLα, a

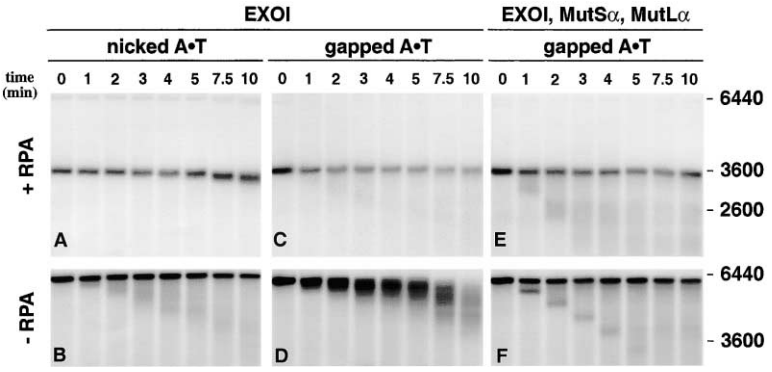

Figure 4. RPA, MutSα, and MutLα Suppress EXOI Excision on Gapped Homoduplex DNA

Kinetics of excision on homoduplex DNA that contained a nick (A and B) or a 314 nucleotide gap (C–F) was examined by indirect end-labeling (see Experimental Procedures and legend to Figure 2). DNAs were analyzed after product cleavage with Bsp106I (A, C, and E) or no digestion (B, D, and F).

(A and B) Reactions contained per time point 24 fmol A•T homoduplex containing a nick at the AccI site and 21 fmol EXOI in the presence (A) or absence (B) of 900 fmol RPA.

(C and D) Reactions were identical to those shown in (A) and (B) except that the homoduplex DNA contained a 314 nucleotide gap extending from the AccI site to the HincII site (Experimental Procedures). The location of the 5′ terminus in this gapped DNA was identical to that of the nicked substrate used in (A) and (B). Incubation was with 21 fmol EXOI in the presence (C) or absence (D) of 900 fmol RPA.

(E and F) Reactions with gapped DNA were as in (C) and (D) but also contained per time point 390 fmol MutSα and 280 fmol MutLα in the presence (E) or absence (F) of 900 fmol RPA.

nicked circular homoduplex is a weak substrate for EXOI hydrolysis, irrespective of the presence of RPA (compare Figures 4A and 4B with Figures 2A and 2B). Figures 4C–4F illustrate the modulatory activities of RPA and the MutSα-MutLα pair on EXOI hydrolysis of gapped circular DNA. In contrast to the weak activity of nicked DNA, gapped DNA was an excellent substrate for EXOI in the absence of other activities (Figure 4D): essentially all molecules were subject to hydrolysis, with products observed after 10 min reduced in length by 400 to 2000 nucleotides. Supplementation of EXOI reactions with RPA rendered a substantial fraction of the gapped molecules resistant to detectable excision by EXOI (compare amounts of undigested material in Figures 4C and 4D), and stabilization afforded by RPA was potentiated 2-fold by MutSα and MutLα (compare Figures 4C and 4E). In the presence of these three proteins, the gapped substrate was largely refractory to EXOI attack, although a small subpopulation of molecules was subject to hydrolysis in a manner similar to that observed in the absence of RPA (Figure 4D). Suppression of hydrolysis on gapped DNA by MutSα and MutLα is also evident in the absence of RPA (Figures 4D and 4F). These findings are consistent with the conclusion discussed above that MutSα and MutLα suppress EXOI activity on mismatch-free DNA.

MutSα Increases EXOI Processivity, and RPA Negatively Regulates This Effect

While MutSα and MutLα suppress EXOI hydrolysis on gapped DNA in the presence or absence of RPA, the nature of the products produced under the two conditions differ (compare Figures 4E and 4F). A particularly striking difference in the distribution of hydrolytic products is also evident in reactions performed in the absence of RPA, depending on whether MutSα and MutLα are present (Figures 4D and 4F). Excision on the subset of gapped molecules that are subject to EXOI attack in the presence of the two proteins yields a quasi-discrete population of hydrolytic products that undergo progressive shortening with time (Figure 4F), whereas hydrolysis of gapped DNA by EXOI alone is more distributive in nature, and essentially all substrate molecules participate in the reaction (Figure 4D). These observations suggested that MutSα and/or MutLα might enhance the processive behavior of EXOI and that RPA may act as a negative regulator of this effect.

These possibilities were confirmed by inhibitor challenge experiments. As shown in Figures 5A and 5B, MutSα, in the absence of MutLα, is sufficient to confer putative processive behavior on EXOI with gapped DNA lacking a mismatch. Supplementation of EXOI reactions with a 2.5-fold molar excess of circular single-stranded f1 DNA abolished hydrolysis of the gapped substrate provided that the inhibitor was present at 0 time, irrespective of the presence of MutSα in the reaction (Figures 5E and 5F). In reactions containing EXOI alone, inhibitor addition 1 min after excision initiation also effectively blocked subsequent hydrolysis (Figure 5D). However, postinitiation addition of the single-strand inhibitor was without significant effect on the progression of hydrolysis that occurred in the presence of MutSα, which continued unabated for several minutes at a rate of 500–550 nucleotides per min (Figure 5C). After removal of about 2000 nucleotides, the product distribution in the presence of inhibitor became diffuse, indicative of dissociation of EXOI, MutSα, or both proteins. Thus, while EXOI digestion of gapped DNA is fairly distributive in nature, MutSα confers processivity on the enzyme permitting removal of several thousand nucleotides per DNA binding event.

A processivity of several thousand nucleotides is seemingly incompatible with the finding described above that in the presence of RPA, MutSα- and mismatch-dependent excision on a nicked heteroduplex terminates upon mismatch removal (Figures 2 and 3). However, RPA is a potent inhibitor of EXOI excision on gapped DNA (Figure 4), and as shown in Figures 5G and 5H, the single-strand binding protein dramatically attenuates the processive behavior of EXOI that occurs in the presence of MutSα. Postinitiation supplementation of processive reactions with RPA largely blocked further excision, and subsequent hydrolysis was limited to about 200–250 nucleotides (mean product size was 3060 nucleotides at 1 min prior to RPA addition as compared to an average size of 2830 nucleotides for 2, 3, and 4 min samples after RPA addition at 1.2 min; Figure 5H). A similar interference of RPA with the processive EXOI action in the presence of MutSα is also evident

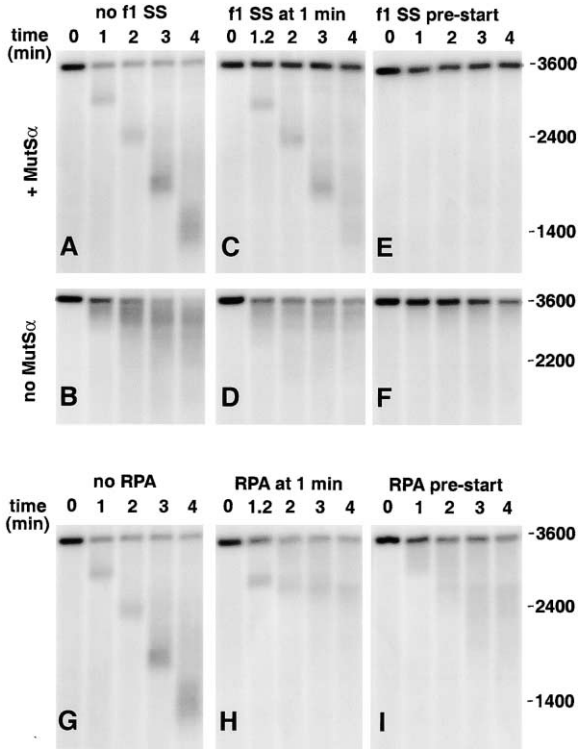

Figure 5. MutSα Renders EXOI Highly Processive, and RPA Negatively Regulates This Effect

(A–F) EXOI hydrolysis on homoduplex DNA containing a 314 nucleotide gap was monitored after Bsp106I cleavage by indirect end-labeling as described in Figures 2 and 4. Reactions contained per time point 24 fmol gapped homoduplex and 21 fmol EXOI in presence (A, C, and E) or absence (B, D, and F) of 390 fmol MutSα. Reactions shown in (E) and (F) were supplemented with f1MR1 circular, single-stranded DNA (60 fmol), an inhibitor of excision, prior to initiation of hydrolysis. Reactions shown in (A) and (B) received no inhibitor, while those shown in (C) and (D) received the single-stranded inhibitor 1 min after initiation of excision. In the presence of MutSα, excision proceeds at approximately 500–550 nucleotides per min as judged by the development of the major excision product with time (A and C).

(G–I) Kinetics of EXOI hydrolysis on gapped DNA in the presence of EXOI and MutSα was determined as in (A) in the absence or presence of 900 fmol RPA. (G) No RPA. (H) RPA added 1 min after initiation of excision. (I) RPA added to reaction prior to initiation of excision. Please note that the initial sample after addition of either single-stranded inhibitor (C) or RPA (H) was taken after 1.2 min.

when the single-strand binding protein was present prior to initiation of the reaction (Figure 5I). The simplest explanation for these observations is that binding of RPA to the growing gap produced by processive excision leads to displacement of EXOI, MutSα, or both proteins from the DNA.

It is noteworthy that the negative regulatory effects of RPA on EXOI processivity are fully consistent with the fact that RPA results in large enhancement in the efficiency of mismatch-provoked excision that occurs in the presence of MutSα, MutLα, and EXOI. In the absence of the single-strand binding protein, excision is restricted to a subset of molecules, which are subject to extensive hydrolysis (Figure 2B). However, the presence of RPA leads to much shorter excision tracts, and displacement of MutSα and/or EXOI from an excision intermediate allows the system to turn over, permitting all of the heteroduplex to participate in the reaction (Figure 2A).

Discussion

The work described here demonstrates that EXOI involvement in 5′-directed mismatch repair is controlled at multiple levels, which are illustrated in the model shown in Figure 6. Although a nick is a poor substrate for the enzyme, EXOI excision at a single-strand break is activated in a MutSα-, mismatch-, and ATP-dependent manner in the presence or absence of RPA. We presume that in the presence of a mismatch cofactor, MutSα facilitates EXOI initiation at a strand break. In contrast to the weak activity of EXOI at a nick, a single-strand gap is an excellent substrate for EXOI attack in the absence of other factors. MutSα renders EXOI excision on gapped DNA highly processive in the absence of RPA, an effect that does not require a mismatch (Figure 4). Since EXOI is known to interact with MSH2 (Tishkoff et al., 1997; Schmutte et al., 1998, 2001; Rasmussen et al., 2000), it seems likely that conferral of processive action on the enzyme reflects existence of a MutSα•EXOI complex on the DNA.

The presence of RPA alters the mechanism of EXOI action, as well as the nature of excision products produced by the enzyme. In the absence of other mismatch repair proteins, the single-strand DNA binding protein suppresses EXOI activity at a gap (Figures 4C and 4D), suggesting that an RPA-filled gap is a weak substrate for the exonuclease as compared to an exposed single-strand region within the helix. RPA also has a striking effect on the mode of action of the MutSα•EXOI complex, dramatically reducing its ability to support processive hydrolysis. This effect suggests that binding of RPA to the growing gap behind the excision complex leads to release of MutSα, EXOI, or both proteins from the helix. As noted above, this permits turnover of the system, allowing all heteroduplex molecules to participate in the reaction. Since the extent of individual processive excision events will be subject to statistical variation, the mechanism shown in Figure 6 predicts variability in excision tract endpoints upon mismatch removal, an effect that has been observed in nuclear extracts (Fang and Modrich, 1993) and in the purified system described here (Figures 2 and 3).

The *E. coli* single-strand binding protein (SSB) can replace RPA in the purified system (see Supplemental Data at http://www.molecule.org/cgi/content/full/12/5/1077/DC1), although the T4 single-strand DNA binding protein is less effective in this regard. The activity of SSB in the purified system indicates that the RPA effects described here are not a consequence of specific interaction of the protein with other components of the excision system. Rather, they suggest that the single-strand binding protein functions by controlling access to the 5′ terminus of a gap by physical occlusion or by modulation of the conformation of the double-strand single-strand junction.

Analysis of mismatched-provoked excision in the MutSα-EXOI-RPA system has indicated occurrence of

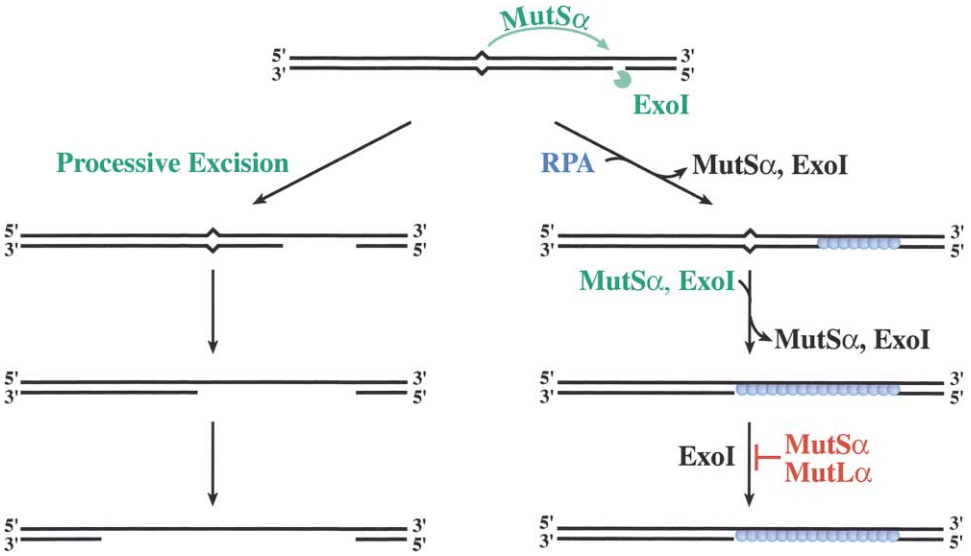

Figure 6. Model for Mismatch-, MutSα-, MutLα-, and RPA-Dependent Modulation of EXOI Activity

EXOI initiates poorly at a single-strand break, and MutSα facilitates this reaction in a mismatch-dependent manner. Once EXOI is loaded by MutSα, excision proceeds in a highly processive manner in the absence of RPA (left diagram). In the presence of RPA (right diagram), the initial gap produced by EXOI is filled by the single-strand binding protein. This results in displacement of EXOI, MutSα, or both proteins from the helix after removal of about 250 nucleotides. Like a single-strand break, an RPA-filled gap is a weak substrate for EXOI, but MutSα promotes reloading of the hydrolytic activity provided that mismatch remains within the DNA. Hence, in the presence of RPA, excision is attenuated upon mismatch removal, and this effect is potentiated by MutSα and MutLα, which further suppress EXOI activity on DNA that lacks a mismatch.

putative excision intermediates (Figures 2 and 3) differing in size by 250 ± 60 nucleotides. Furthermore, excision continues for about 200–250 nucleotides after RPA supplementation of reactions in which processive excision is ongoing (Figure 5H). On the basis of these observations, we infer that in the presence of RPA, the MutSα•EXOI complex removes about 250 nucleotides prior to dissociation, but this number could vary depending on sequence context and other factors. Although the resulting RPA-filled gap is a poor substrate for EXOI, our finding that the purified system supports efficient mismatch removal from molecules with a nick-mismatch separation as large as 808 base pairs (Figure 3) implies that MutSα can facilitate EXOI reloading at an RPA-filled gap as long as a mismatch cofactor remains within the molecule. However, once the mismatch is removed, the efficiency of excision drops dramatically because MutSα can no longer activate the exonuclease. We have also shown that MutSα and MutLα suppress EXOI activity on mismatch-free DNA containing an RPA-filled gap (Figure 4). This negative regulatory effect further attenuates the weak substrate activity of an RPA-filled gap in a mismatch-free molecule, resulting in effective termination of excision upon mismatch removal.

The polarity of the mismatch-, MutSα-, MutLα-, RPA-, and EXOI-dependent excision reaction described here is exclusively 5′ to 3′, consistent with the reported 5′ to 3′ polarity of yeast and human EXOI (Szankasi and Smith, 1992; Tishkoff et al., 1997; Wilson et al., 1998). While this reaction can account for excision directed by a 5′ strand break, previous analysis of depleted nuclear extracts has shown that EXOI is also required for excision directed by a strand break located 3′ to the mispair (Genschel et al., 2002). This observation indicates that the 5′ to 3′ hydrolytic activity of EXOI must be regulated in a manner that depends on the relative orientation of the strand signal and the mispair: the 5′ to 3′ hydrolytic activity of EXOI will be activated when the strand break resides 5′ to the mismatch but must be suppressed when the nick resides 3′ to the mispair. This implies existence of additional factors that regulate EXOI activity when mismatch-provoked excision is directed by a 3′ strand break. We are currently pursuing the identity of these activities.

Although previous work with nuclear extracts has implicated MutLα and PCNA in mismatch-provoked excision (Umar et al., 1996), PCNA is not required for 5′ to 3′ excision in the purified system described here, and MutLα participation is restricted to enhancement of the mismatch specificity of the reaction. To further clarify the roles of these two proteins in mismatch repair, we have reassessed their involvement in the nuclear extract reaction. We have found that the peptide corresponding to the $p21^{WAF1}$ element that interacts with PCNA abolishes excision directed by a 3′ strand break (see Supplemental Data), confirming previous observations (Umar et al., 1996); however, the peptide reduced 5′-directed excision to a limiting value of only 50%, implying that PCNA is not essential for excision directed by a 5′ strand signal, consistent with the purified system. While the modest inhibition in the extract system may indicate a significant role for PCNA in 5′ excision, this limited effect could also be an indirect consequence of PCNA suppression of competing reactions that may otherwise occur on a 5′ heteroduplex in crude fractions. Such effects would not be evident in the purified system. It is also noteworthy that, with one exception, all of the experimental data initially implicating PCNA in mismatch-pro-

voked excision was obtained using 3′ heteroduplexes (Umar et al., 1996).

We have also found that immunodepletion of MutLα abolishes mismatch-provoked excision when the reaction is directed by a 3′ strand break but is without significant effect on excision directed by a 5′ nick (see Supplemental Data), again consistent with results obtained with the purified system. Indeed, previous analyses of MutLα deficient human tumor cell lines have yielded disparate results with respect to the MutLα requirement for repair directed by a 5′ strand break. For example, extracts derived from the colorectal tumor cell line HCT116 (and its subclone H6), which harbors chain terminator mutations in both MLH1 alleles (Papadopoulos et al., 1994), are deficient in mismatch repair directed by a 3′ or 5′ strand break. Supplementation with exogenous MutLα restores 3′ and 5′ repair to normal levels (Li and Modrich, 1995). By contrast, several other cell lines that are MutLα-deficient due to epigenetic silencing of *MLH1* loci by promoter methylation (Kane et al., 1997; Herman et al., 1998; Veigl et al., 1998; Strathdee et al., 1999) behave differently. Extracts prepared from these cell lines are defective in the correction of 3′ heteroduplexes but display near normal levels of 5′ heteroduplex repair (Drummond et al., 1996; G.-M. Li, J. Drummond, L. Bazemore, S. Littman, and P.M., unpublished data). While the molecular bases of these cell line differences have not been established, we have suggested that this disparity may be due to sequestration of a required 3′ repair component by fragments of the MLH1 polypeptide present in the HCT116 cell line (Genschel et al., 2002). The cell lines in which the MLH1 loci are epigenetically silenced are devoid of MLH1 crossreacting material.

Experimental Procedures

Proteins and Nuclear Extract

HeLa nuclear extract was prepared (Genschel et al., 2002), MutSα isolated from HeLa cells (Drummond et al., 1995), and MutLα and EXOI prepared from baculovirus-infected insect cells (Blackwell et al., 2001; Genschel et al., 2002) as described previously. RPA was purified from an *E. coli* overproducer as described (Henricksen et al., 1994) and further purified by chromatography on a 1 ml MonoQ column (HR 5/5, Amersham Biosciences) equilibrated with 25 mM HEPES-KOH (pH 7.5), 0.1 mM EDTA, 0.1 M KCl. The column was developed with a gradient of 0.1 to 0.37 M KCl. RPA-containing fractions were pooled, quick-frozen in liquid nitrogen, and stored at −80°C. Protein concentrations were determined by Bradford assay using bovine serum albumin as standard.

Mismatch Repair and Gap Formation Assays

Mismatch repair substrates were prepared from f1MR phage, and mismatch repair and gap formation (dNTPs omitted) assays performed as described previously (Fang and Modrich, 1993; Genschel et al., 2002). Heteroduplex/homoduplex DNAs contained a G-T mismatch or A•T base pair at position 5632 and a single-strand break in the complementary DNA strand at the Sau96I, AccI, or HincII sites. The strand break in these molecules was 5′ to the mispair, with nick-mismatch separation distances of 128, 494, or 808 base pairs as viewed along the shorter path joining the two sites in the circular substrate. Gapped circular DNAs were similar to nicked homoduplex DNAs but contained a 314 nucleotide gap between the AccI and HincII sites of the complementary strand.

Proteins were diluted as necessary into 7.5 mM HEPES-KOH (pH 7.5), 200 mM KCl, 0.6 mM dithiothreitol, 2 mg/ml bovine serum albumin, 10% (vol/vol) glycerol. Reactions with purified proteins were assembled by mixing indicated proteins in a total volume of 10 μl of dilution buffer with 10 μl of 40 mM Tris-HCl (pH 7.6), 3 mM ATP, 2 mM glutathione, 10 mM $MgCl_2$, 0.1 mg/ml bovine serum albumin, 2.4 nM heteroduplex/homoduplex DNA. If not specified, mismatch-provoked excision reactions were incubated 5 min at 37°C. For single point reactions, components were placed as individual droplets on the wall of a 1.5 ml centrifuge tube at 0°C. After mixing of components by a quick spin in an Eppendorf centrifuge, tubes were transferred to 37°C. For time course reactions, all components except EXOI were combined on ice and incubated at 37°C for 1 min. Excision was then initiated by EXOI addition.

Indirect End-Labeling

Excision tracts were analyzed by indirect end-labeling (Fang and Modrich, 1993; Genschel et al., 2002). DNA recovered from gap formation assays was digested with Bsp106I as indicated, and products were resolved by electrophoresis through 1% agarose in 50 mM NaOH, 1 mM EDTA for 500 V · hr (Fang and Modrich, 1993; Genschel et al., 2002). After transfer to nylon membranes (Hybond N+, Amersham Biosciences), DNA was probed with ^{32}P-labeled synthetic oligonucleotides complementary to the incised strand of the substrate. For DNAs cleaved with Bsp106I prior to analysis, the probe corresponded to viral strand nucleotides 2532–2552. When products were analyzed without Bsp106I cleavage, probes were as follows: heteroduplex/homoduplex DNAs containing a nick at the Sau96I site (viral strand nucleotides 5761–5777), homoduplex DNA with a nick at the AccI site (viral strand nucleotides 6138–6154), homoduplex DNA with a gap extending from the AccI to HincII site (viral strand nucleotides 1–24).

Acknowledgments

This work was supported in part by grants R01-GM45190 and P01-CA92584 from the National Institutes of Health. P.M. is an Investigator of the Howard Hughes Medical Institute.

Received: November 27, 2002
Revised: October 8, 2003
Accepted: October 8, 2003
Published: November 20, 2003

References

Amin, N.S., Nguyen, M.N., Oh, S., and Kolodner, R.D. (2001). *exo1*-dependent mutator mutations: model system for studying functional interactions in mismatch repair. Mol. Cell. Biol. *21*, 5142–5155.

Au, K.G., Welsh, K., and Modrich, P. (1992). Initiation of methyl-directed mismatch repair. J. Biol. Chem. *267*, 12142–12148.

Blackwell, L.J., Martik, D., Bjornson, K.P., Bjornson, E.S., and Modrich, P. (1998). Nucleotide-promoted release of hMutSα from heteroduplex DNA is consistent with an ATP-dependent translocation mechanism. J. Biol. Chem. *273*, 32055–32062.

Blackwell, L.J., Wang, S., and Modrich, P. (2001). DNA chain length dependence of formation and dynamics of hMutSα•hMutLα•heteroduplex complexes. J. Biol. Chem. *276*, 33233–33240.

Buermeyer, A.B., Deschenes, S.M., Baker, S.M., and Liskay, R.M. (1999). Mammalian DNA mismatch repair. Annu. Rev. Genet. *33*, 533–564.

Cooper, D.L., Lahue, R.S., and Modrich, P. (1993). Methyl-directed mismatch repair is bidirectional. J. Biol. Chem. *268*, 11823–11829.

Dao, V., and Modrich, P. (1998). Mismatch, MutS, MutL, and helicase II-dependent unwinding from the single-strand break of an incised heteroduplex. J. Biol. Chem. *273*, 9202–9207.

Drummond, J.T., Li, G.-M., Longley, M.J., and Modrich, P. (1995). Isolation of an hMSH2•p160 heterodimer that restores mismatch repair to tumor cells. Science *268*, 1909–1912.

Drummond, J.T., Anthoney, A., Brown, R., and Modrich, P. (1996). Cisplatin and adriamycin resistance are associated with MutLα and mismatch repair deficiency in an ovarian tumor cell line. J. Biol. Chem. *271*, 19645–19648.

Ellis, L.A., Taylor, G.R., and Baumberg, S. (1994). MutS binding protects heteroduplex DNA from exonuclease digestion in vitro: a

simple method for detecting mutations. Nucleic Acids Res. *22*, 2710–2711.

Fang, W.-h., and Modrich, P. (1993). Human strand-specific mismatch repair occurs by a bidirectional mechanism similar to that of the bacterial reaction. J. Biol. Chem. *268*, 11838–11844.

Genschel, J., Bazemore, L.R., and Modrich, P. (2002). Human exonuclease I is required for 5′ and 3′ mismatch repair. J. Biol. Chem. *277*, 13302–13311.

Gradia, S., Subramanian, D., Wilson, T., Acharya, S., Makhov, A., Griffith, J., and Fishel, R. (1999). hMSH2-hMSH6 forms a hydrolysis-independent sliding clamp on mismatched DNA. Mol. Cell *3*, 255–261.

Harfe, B.D., and Jinks-Robertson, S. (2000). DNA mismatch repair and genetic instability. Annu. Rev. Genet. *34*, 359–399.

Henricksen, L.A., Umbricht, C.B., and Wold, M.S. (1994). Recombinant replication protein A: expression, complex formation, and functional characterization. J. Biol. Chem. *269*, 11121–11132.

Herman, J.G., Umar, A., Polyak, K., Graff, J.R., Ahuja, N., Issa, J.P., Markowitz, S., Willson, J.K., Hamilton, S.R., Kinzler, K.W., et al. (1998). Incidence and functional consequences of hMLH1 promoter hypermethylation in colorectal carcinoma. Proc. Natl. Acad. Sci. USA *95*, 6870–6875.

Jager, A.C., Rasmussen, M., Bisgaard, H.C., Singh, K.K., Nielsen, F.C., and Rasmussen, L.J. (2001). HNPCC mutations in the human DNA mismatch repair gene hMLH1 influence assembly of hMutL-alpha and hMLH1-hEXO1 complexes. Oncogene *20*, 3590–3595.

Jagmohan-Changur, S., Poikonen, T., Vilkki, S., Launonen, V., Wikman, F., Orntoft, T.F., Moller, P., Vasen, H., Tops, C., Kolodner, R.D., et al. (2003). EXO1 variants occur commonly in normal population: evidence against a role in hereditary nonpolyposis colorectal cancer. Cancer Res. *63*, 154–158.

Jiricny, J. (1998). Eukaryotic mismatch repair: an update. Mutat. Res. *409*, 107–121.

Kane, M.F., Loda, M., Gaida, G.M., Lipman, J., Mishra, R., Goldman, H., Jessup, J.M., and Kolodner, R. (1997). Methylation of the hMLH1 promoter correlates with lack of expression of hMLH1 in sporadic colon tumors and mismatch repair-defective human tumor cell lines. Cancer Res. *57*, 808–811.

Kolodner, R. (1996). Biochemistry and genetics of eukaryotic mismatch repair. Genes Dev. *10*, 1433–1442.

Li, G.-M., and Modrich, P. (1995). Restoration of mismatch repair to nuclear extracts of H6 colorectal tumor cells by a heterodimer of human MutL homologs. Proc. Natl. Acad. Sci. USA *92*, 1950–1954.

Modrich, P., and Lahue, R. (1996). Mismatch repair in replication fidelity, genetic recombination, and cancer biology. Annu. Rev. Biochem. *65*, 101–133.

Papadopoulos, N., Nicolaides, N.C., Wei, Y.-F., Ruben, S.M., Carter, K.C., Rosen, C.A., Haseltine, W.A., Fleischmann, R.D., Fraser, C.M., Adams, M.D., et al. (1994). Mutation of a *mutL* homolog in hereditary colon cancer. Science *263*, 1625–1629.

Ramilo, C., Gu, L., Guo, S., Zhang, X., Patrick, S.M., Turchi, J.J., and Li, G.M. (2002). Partial reconstitution of human DNA mismatch repair in vitro: characterization of the role of human replication protein A. Mol. Cell. Biol. *22*, 2037–2046.

Rasmussen, L.J., Rasmussen, M., Lee, B., Rasmussen, A.K., Wilson, D.M., Nielsen, F.C., and Bisgaard, H.C. (2000). Identification of factors interacting with hMSH2 in the fetal liver utilizing the yeast two-hybrid system. In vivo interaction through the C-terminal domains of hEXO1 and hMSH2 and comparative expression analysis. Mutat. Res. *460*, 41–52.

Schmutte, C., Marinescu, R.C., Sadoff, M.M., Guerrette, S., Overhauser, J., and Fishel, R. (1998). Human exonuclease I interacts with the mismatch repair protein hMSH2. Cancer Res. *58*, 4537–4542.

Schmutte, C., Sadoff, M.M., Shim, K.S., Acharya, S., and Fishel, R. (2001). The interaction of DNA mismatch repair proteins with human exonuclease I. J. Biol. Chem. *276*, 33011–33018.

Sokolsky, T., and Alani, E. (2000). EXO1 and MSH6 are high-copy suppressors of conditional mutations in the MSH2 mismatch repair gene of Saccharomyces cerevisiae. Genetics *155*, 589–599.

Strathdee, G., MacKean, M.J., Illand, M., and Brown, R. (1999). A role for methylation of the hMLH1 promoter in loss of hMLH1 expression and drug resistance in ovarian cancer. Oncogene *18*, 2335–2341.

Sun, X., Zheng, L., and Shen, B. (2002). Functional alterations of human exonuclease 1 mutants identified in atypical hereditary nonpolyposis colorectal cancer syndrome. Cancer Res. *62*, 6026–6030.

Szankasi, P., and Smith, G.R. (1992). A DNA exonuclease induced during meiosis of Schizosaccharomyces pombe. J. Biol. Chem. *267*, 3014–3023.

Tishkoff, D.X., Boerger, A.L., Bertrand, P., Filosi, N., Gaida, G.M., Kane, M.F., and Kolodner, R.D. (1997). Identification and characterization of Saccharomyces cerevisiae EXO1, a gene encoding an exonuclease that interacts with MSH2. Proc. Natl. Acad. Sci. USA *94*, 7487–7492.

Tishkoff, D.X., Amin, N.S., Viars, C.S., Arden, K.C., and Kolodner, R.D. (1998). Identification of a human gene encoding a homologue of Saccharomyces cerevisiae EXO1, an exonuclease implicated in mismatch repair and recombination. Cancer Res. *58*, 5027–5031.

Tran, P.T., Simon, J.A., and Liskay, R.M. (2001). Interactions of Exo1p with components of MutLalpha in *Saccharomyces cerevisiae*. Proc. Natl. Acad. Sci. USA *98*, 9760–9765.

Umar, A., Buermeyer, A.B., Simon, J.A., Thomas, D.C., Clark, A.B., Liskay, R.M., and Kunkel, T.A. (1996). Requirement for PCNA in DNA mismatch repair at a step preceding DNA resynthesis. Cell *87*, 65–73.

Veigl, M.L., Kasturi, L., Olechnowicz, J., Ma, A.H., Lutterbaugh, J.D., Periyasamy, S., Li, G.M., Drummond, J., Modrich, P.L., Sedwick, W.D., and Markowitz, S.D. (1998). Biallelic inactivation of hMLH1 by epigenetic gene silencing, a novel mechanism causing human MSI cancers. Proc. Natl. Acad. Sci. USA *95*, 8698–8702.

Viswanathan, M., Burdett, V., Baitinger, C., Modrich, P., and Lovett, S.T. (2001). Redundant exonuclease involvement in *Escherichia coli* methyl-directed mismatch repair. J. Biol. Chem. *276*, 31053–31058.

Wang, H., and Hays, J.B. (2002). Mismatch repair in human nuclear extracts. Quantitative analyses of excision of nicked circular mismatched DNA substrates, constructed by a new technique employing synthetic oligonucleotides. J. Biol. Chem. *277*, 26136–26142.

Wei, K., Clark, A.B., Wong, E., Kane, M.F., Mazur, D.J., Parris, T., Kolas, N.K., Russell, R., Hou, H., Jr., Kneitz, B., et al. (2003). Inactivation of exonuclease 1 in mice results in DNA mismatch repair defects, increased cancer susceptibility, and male and female sterility. Genes Dev. *17*, 603–614.

Wilson, D.M., III, Carney, J.P., Coleman, M.A., Adamson, A.W., Christensen, M., and Lamerdin, J.E. (1998). Hex1: a new human Rad2 nuclease family member with homology to yeast exonuclease 1. Nucleic Acids Res. *26*, 3762–3768.

Wu, Y., Berends, M.J., Post, J.G., Mensink, R.G., Verlind, E., Van Der Sluis, T., Kempinga, C., Sijmons, R.H., van der Zee, A.G., Hollema, H., et al. (2001). Germline mutations of EXO1 gene in patients with hereditary nonpolyposis colorectal cancer (HNPCC) and atypical HNPCC forms. Gastroenterology *120*, 1580–1587.